*Research Journal of Physical Sciences* ISSN 2320–4796
Vol. **10(1),** 1-7, February **(2022)** *Res. J. Physical Sci.*

# Two far infrared cavities nearby asymptotic giant branch stars at the galactic plane

**Gautam A.K.* and Aryal B.**
[1]Bhaktapur Multiple Campus, Tribhuvan University, Bhaktapur, Nepal
[2]Central Department of Physics, Tribhuvan University, Kirtipur, Nepal
arjungautamnpj@gmail.com

**Available online at: www.isca.in, www.isca.me**
Received 30th April 2021, revised 24th October 2021, accepted 10th January 2022

## Abstract

*Dust color temperature, Planck function, visual extinction and their distributions of two far infrared cavities (named FIC06+00 and FIC21+48) found to be located within $3^0$ around the AGB stars namely AGB0651+0031 and AGB2129+4919 at the galactic plane are presented. Dust color temperature of the core region of the cavities are found to be (20.5±1.2) K to (22.0±0.8) K and (22.1±0.1) K to (22.6±0.4) K respectively. The product of dust color temperature and visual extinction is found to be consistent in the order of $10^{-4}$. The distribution of Planck function along the extension (major diameter) and compression (minor diameter) is found to be non-uniform means dust particles are oscillating sinusoidally in order to get dynamical equilibrium which may be the cause of grain temperature. It further suggests that the dust particles in the cavities might not be in the thermal equilibrium possibly due to pressure driven events specially nearby AGB stars. Negative slope in transition from 25 μm to 60μm is our finding regarding far infrared spectral distribution in the cavities. It suggests that the number density of dust particles are found to be less than expected in 60 μm region.*

**Keywords:** ISM, AGB Star, Dust, IRAS, Visual Extinction.

## Introduction

An asymptotic giant branch (AGB) star is generally believed to be in the last evolutionary phases of a low and intermediate mass star ($M \leq 10M_{\odot}$). Most of the AGB stars can be identified as long-period variables (LPVs) with large amplitude pulsation. The strong pulsation produces shock waves which extend the outer layer of an AGB star for better condition of dust formation[1]. Newly dust grains may drive dusty stellar winds with high mass loss rates of $10^{-8} - 10^{-4}M_{\odot}$/yr due to radiation pressure produced[2]. Due to such dusty stellar winds and evolution of the central stars during the AGB phase, the cool and slowly expanding (10−30km $s^{-1}$) dust envelopes surrounding AGB stars are formed. AGB stars are believed to be the main source of major stellar objects which are able to significantly affect the integrated spectral energy distributions of star clusters and galaxies[3]. The asymptotic giant branch (AGB) phase is the final nuclear burning stellar evolutionary stage of low and intermediate mass (1–8 $M_{\odot}$) stars and this stage is characterized by low surface effective temperatures (∼2000-3500K), high luminosity(∼1000-10,000 $L_{\odot}$), intense mass loss (from $10^{-7}$ to $10^{-4}$ $M_{\odot}yr^{-1}$)[4]. AGB stars are final nuclear burning stage of low and intermediate mass stars which may be considered as the primary source of dust in the interstellar medium (ISM)[5]. AGB wind interacts directly with the ISM because Low mass stars do not have a strong wind until they reach the AGB phase. The AGB wind interacts directly with the ISM, rather than with the stellar wind remnants from earlier evolutionary stages, as would be the case for more massive stars[6]. The collision between the stellar wind and the ISM results in the formation of a high density shell of swept-up interstellar gas, which is pushed outwards into the ISM. On the basis of degenerate core, AGB stars which are classified in to oxygen- rich (M-type) and carbon-rich (C-type)[5]. But in the catalog provided by Suh & Kwon[7], (AGB) stars are classified into four types: O-rich stars (M-type Miras and OH = IR stars), C-rich stars (C-type stars or carbon stars), S stars, and silicate carbon stars. They presented the catalog of 2193 O-rich stars, 1167 C-rich stars, 287 S stars and 36 silicate carbon stars.

The AGB star and its surroundings is the natural laboratory in which its effect in the interstellar medium can be studied. A catalog of AGB stars in IRAS PSC was developed where they were classified with coordinates of individual AGB stars which was the initial stage to find far infrared cavities nearby the AGB stars[7]. Two giant bi polar dust emission structures centred on PNNGC1514 at FIR wavelengths was found[8]. In another work, the PN NGC 2899 was located at the center of a huge quadrupolar cavity, whose directions of axes coincide with the directions of the main axes of the optical PN was noticed[9]. A new infrared nebula (R.A. = 08h 27m, Dec. =+250 54' (J2000) was detected)[10], suggested that the pulsar PSRB0823+26 might be responsible for its shaping.

Dust color temperature inside and outside of four far infrared loops nearby pulsars located within $1^0$ was presented by authors[11]. The measured dust color temperature of the core region was in the range (19.4±1.2) K to (25.3±1.7) K, where as

the range increased to (33±2) K to (47±3) K for the outer region. For this work, similar method for calculation of dust color temperature and Planck function has been used. In another study, dust color temperature of two far-infrared cavities was calculated using AKARI and IRIS maps[12]. Interestingly, they found that the longer wavelength AKARI map gives larger values of dust color temperature than that of the shorter wavelength IRIS maps.

**Far Infrared Cavities:** Infrared two-colour diagrams were presented[7] and found 3003 O-rich, 1168 C-rich, 362 S-type and 35 silicate carbon stars in our Galaxy. To find far infrared cavities around the 1168 C-rich AGB stars at 60 and 100µm IRIS maps, a systematic search was performed by using Sky View Virtual Observatory, and selected two far infrared cavities for the study. For the selection of the cavities, following criteria were maintained: (i) the core region of the cavity should have minimum flux at 100µm IRIS maps, (ii) the major diameter should be > $0.3^0$ (iii) should be located within $3^0$ of C-rich AGB stars, (iv) should lie in the Galactic plane ($-2^0 < b < 0^0$), and (v) there should be no diffuse optical emission. The database of two far infrared (FIR) cavities is listed in Table-1. In the present work, it is intended to study flux density at four bands i.e., 12, 25, 60 and 100 micron wavelength. Dust color temperature, visual extinction and the distribution of Planck function along the compression and extension of the cavities are measured and analysed. Finally, nature of FIR spectral distribution of the cavities are also studied.

In this paper, the physical properties of two far infrared cavities found during systematic search on IRAS maps, located close to the AGB stars are studied. Selection criteria for the cavities are previously described. Methods of calculation, brief description of the result and discussion are discussed in separate sections and finally results are concluded in the section conclusion.

## Materials and methods

Two far infrared cavities under 60 and 100 micron IRAS maps around the carbon-rich AGB stars were found. For calculation of dust color temperature, Planck function and visual extinction of the dusty environment around the Asymptotic Giant Branch stars, a method is briefly described. For it, we used the method of calculation for the dust color temperature and the Planck function were described Jha, A. K. et. al[11].

**Dust Color Temperature:** The dust color temperature of all pixels of selected two FIR cavities were calculated using 60 and 100µm IRAS flux densities. For it, there is a simple and frequently used method[13], and later it was improved by many authors[14,15]. Finally, the derived expression for dust color temperature $T_d$ is written as

$$T_d = \frac{-96}{\ln\{R \times 0.6^{(3+\beta)}\}}, \qquad \text{where , } R = \frac{F(60\mu m)}{F(100\mu m)} \qquad (1)$$

Here, β is the spectral emissivity index which depends on dust grain properties like composition, size, and compactness. β = 0, for a pure blackbody, β ~ 1, for the amorphous layer-lattice matter and β ~ 2 for the metals and crystalline dielectrics. For this work, β ~ 2 has been used in the calculations.

Here, F (60µm) and F (100µm) are the flux densities in 60µm and 100 µm respectively and Equation (1) can be used for calculation of the dust color temperature.

**Planck Function:** The value of Planck function depends on the wavelength (frequency), and hence dust color temperature. For calculation, formula for the Planck function is given by[16]**,**

$$B(\nu,T) = \frac{2h\nu^3}{c^2}\left(\frac{1}{e^{\frac{h\nu}{kT}} - 1}\right) \qquad (2)$$

where, h = Planck constant, c = velocity of light, ν = frequency at which the emission is observed, T = the average dust color temperature of the region.

From Equation (2), it is clear from the expression that the value of Planck function B(ν, T) for longer wavelength is higher than that of the shorter wavelength. Consequently, the range of B (ν, T) for fixed temperature (say ΔT) goes narrower if wavelength of the images increases.

**Table-1:** The database of two far infrared cavities nearby AGB stars at the galactic plane. The first column represents name (FIChh+dd). The second and third columns give positions. The next two columns list the major (a) and minor (b) diameters of the cavities. The last column lists the name of nearby AGB star.

| FIC | α(J2000) (deg) | δ(J2000) (deg) | a (deg) | b (deg) | Nearby AGB |
|---|---|---|---|---|---|
| FIC06+00 | 06h 49m 47.1s | $00^0$ 31' 32.4" | 0.4 | 0.2 | AGB0651+0031 |
| FIC21+48 | 21h 31m 53.7s | $48^0$ 59' 07.5" | 0.3 | 0.2 | AGB2129+4919 |

**Visual Extinction:** For estimation of visual extinction of the core region of the cavities, an empirical formula was provided[12]. According to them, the formula is written as is optical depth at 100μm wavelength. Here $F_\lambda$ is flux density and $B_\lambda$ is Planck function at 100μm wavelength.

$$A_v(\text{mag}) = 15.078\,[1 - \exp(-\tau_{100}/641.3)] \quad (3)$$

$$\text{where, } \tau_{100} = \frac{F_\lambda(100\text{ mm})}{B_\lambda(100\text{ mm}, T_d)} \quad (4)$$

## Results and Discussion

We describe the physical properties of two FIR cavity candidates and compare them with the previously published works.

**FIC06+00:** The cavity FIC06+00 was located at R.A. (J2000) = 06h 49m 47.1s, Dec.(J2000)= $00^0$ 32' 32.4" (l =$212.3^0$ and b = $-0.1^0$). The cavity was elongated along north-south direction and compressed along east-west direction. Size of the cavity and position angle were found to be 0.40×0.20 and $297.1^0$ respectively. Figure-1(a) shows the cavity FIC06+00 at 100μm IRIS map. There were 132 pixels in the region of interest. The values of flux densities at 12μm, 25μm, 60μm and 100μm were obtained by using FITS images in the ALADIN2.5 software. Flux densities at 60μm versus 100μm were plotted in Figure-1(b). The slope of best fit line was used to calculate the errors in the calculation of dust color temperature. Dust color temperature ($T_d$) of each pixel was calculated by using Equation-(1) and found in the range (20.5±1.2) K to (22.0±0.8) K. In the dust color temperature map, Figure-1(c), the central region showed north-south elongation representing region of temperature minima. Figure-1(d) showed distribution of dust color temperature of the cavity and found to be deviated from the Gaussian distribution. It showed positive skewness means more data are distributed in left sides. It is due to strong role of nearby AGB stars in the formation of cavity. Figures-1(e,f) showed the variation of Planck function along the extension (major diameter passing through flux minima at 100μm) and compression (minor diameter passing through flux minima at 100μm) of the cavity. It showed that Planck function was not distributed uniformly. It means, observed distribution of Planck function was found to be fluctuating non-uniformly along both major and minor diameters, suggesting sinusoidal distribution.

$$B(\lambda,T) = B_0 + A \sin\left(\pi \frac{D - D_c}{\omega}\right) \quad (5)$$

where $B_0$, A, $D_c$ and ω represent offset, amplitude (A > 0), phase shift and period, respectively. In both cavities, the values of $B_0$, A, $D_c$ and ω for major and minor diameters are shown in the Figures-1(e,f). On comparing Figures-1(c,g) to each other, it is found that higher the dust color temperature , lower the visual extinction and vice-versa. Such type of behavior was also noticed [17]. Figure-1(h) showed a systematic trend with excellent correlation coefficient between dust color temperature and visual extinction. Graphically, product of visual extinction and dust color temperature was found to be $1.0\times10^{-4}$ K mag which is very close to the calculated value.

**FIC21+48:** The cavity FIC21+48 is located at R.A. (J2000) = 21h 32m 19.36s, Dec. (J2000) = $48^0$ 43' 54.7" (l=$92.7^0$ and b = $-1.3^0$) with $43.5^0$ position angle. Figure-2(a) showed the cavity FIC21+48 at 100μm IRIS map. There were 90 pixels in the region of interest. The values of flux densities at 60μm and 100 μm are obtained by FITS image of the field using ALADIN2.5 software. A scattering plot between flux density at 60 μm and 100μm has shown in Figure-2(b). The slope of best fit was used to calculate the errors in the value of dust color temperature. Equation-(1) is used to calculate dust color temperature ($T_d$) of each pixel of the cavities and found in the range (22.1±0.1) K to (22.6±0.4) suggesting that the cavities are in thermal isolation. In the dust color temperature map, Figure-2(c), minimum temperature region was found to lie at the boundary of north-west part where as maximum temperature region lain at the eastern part of the cavity with north-south elongation. Figure-2(d) showed dust color temperature distribution in the cavity. This distribution was found to be Gaussian like distribution means temperature distribution supports natural behavior. Figures-2(e,f) showed the variation of Planck function along the extension and compression of the cavity. It showed that Planck function was distributed non-uniformly. Since the observed distribution of Planck function was found to be fluctuating non-uniformly along both major and minor diameters hence similar sinusoidal distribution as described in Equation-(5) was found.

In both cavities, the values of $B^0$, A, $D^c$ and ω for major and minor diameters are shown in the Figure-2(e ,f). When Figures-2(c,g) are compared, they show higher the dust color temperature, lower the visual extinction and vice-versa.. Figure-2(h) showed a systematic trend with moderate correlation coefficient between them. Here, product of visual extinction and dust color temperature was found to be $1.2\times10^{-4}$ K mag which is very close to the calculated value.

The variation of wavelengths with their flux densities is called spectral distribution. The spectral distribution of the two far infrared cavities is shown in Figure-3. In one cavity, a significant rise from 12μm to 25μm and then a fall from 25μm to 60 μm was noticed but in another cavity, continuous increase in flux density with increase in wavelength was noticed. When comparing with the cavities studied[17], a similar trend was noticed for cavity FIC05+00. But cavity FIC21+48 showed like skeleton nebula[10] and MBM cloud[18]. A continuous rise with different slope was noticed for these nebula. It means, one FIR cavity emits less radiation at 60μm wavelengths than that of the nebular cavity. It suggests that the deficiency of materials (dust and grain) in the FIR cavities. These materials are expected to be swept away from the cavity due to AGB wind.

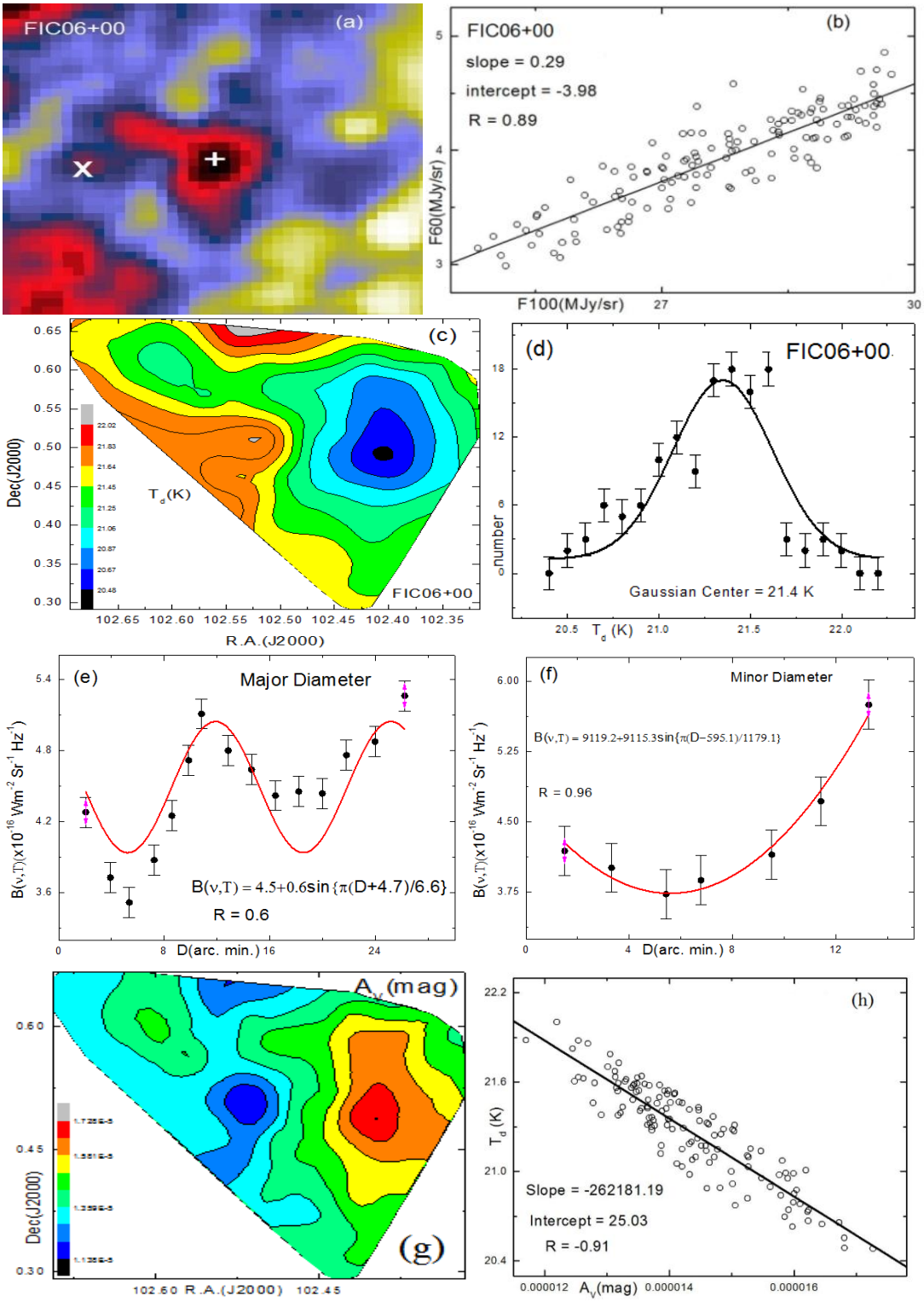


**Figure-1:** (a) JPEG image at 100 μm wavelength of the far infrared cavity FIC06+00 centered at R.A. (J2000) = 06h 49m 47.1s, Dec (J2000) = $00^0$ 31' 32.4". The symbol '+' represents the central position of the cavity and symbol '×' represents the position of the AGB star (AGB06+00). (b) Flux at 100μm versus 60 μm plot. (c,g) are contour map of dust color temperature and visual extinction. The contour levels are shown. The best fit equations are given (error in parentis). The distribution of Planck function along the extension (major diameter) (e) and compression (minor diameter) (f) of the cavity. The solid curves represent Gaussian (d), sine curve fitted (e,f) and linear fitted line (b,h).

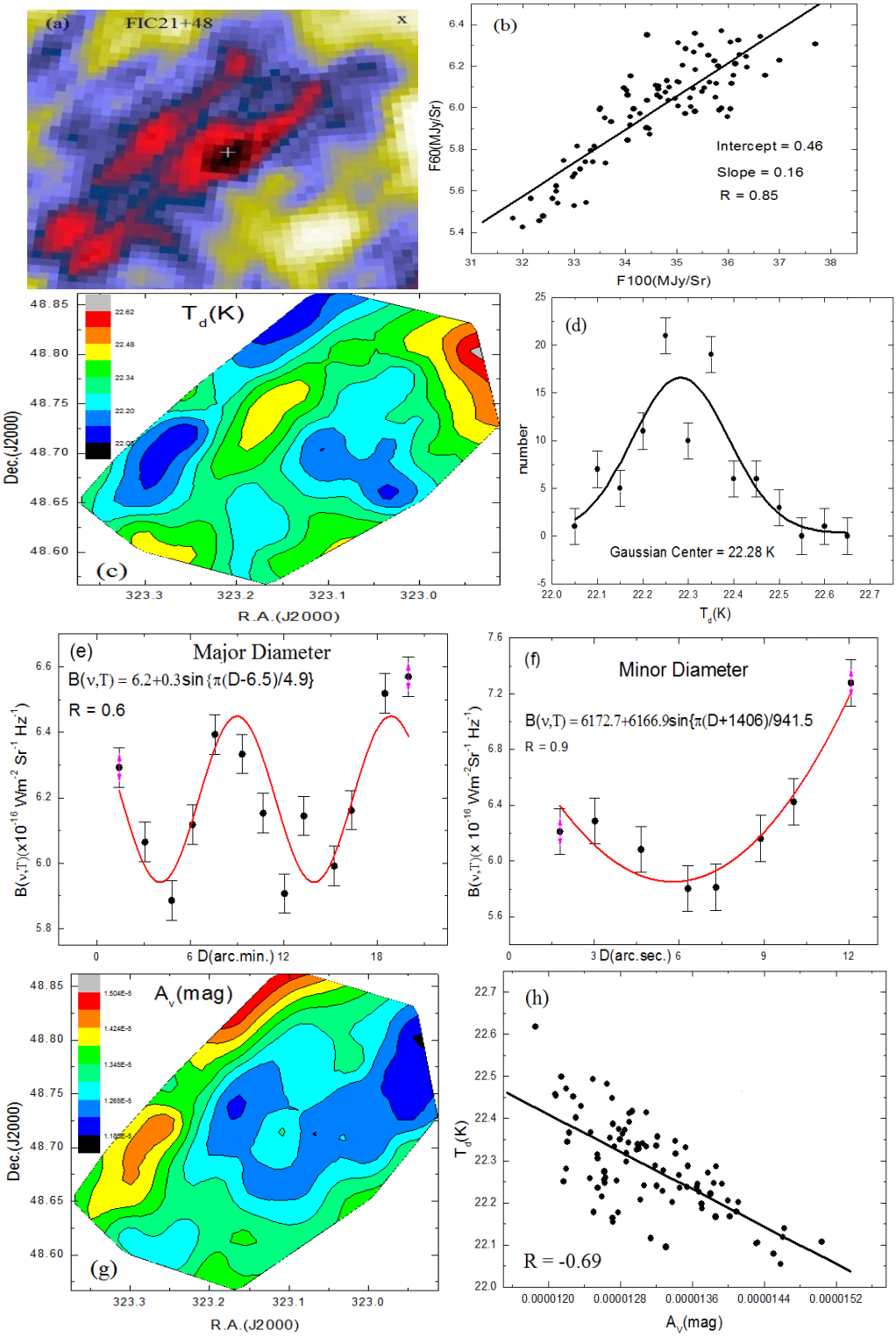


**Figure-2:** (a) JPEG image at 100µm wavelength of the far infrared cavity FIC21+48 centered at R.A. (J2000) = 21h 32m 19.36s, Dec. (J2000) =48$^0$ 43' 54.7". The symbol '+' represents the central position of the cavity and symbol '×' represents the position of the AGB star (AGB2129+4919). (b) Flux at 100µm versus 60µm plot. (c,g) are contour maps of dust color temperature and visual extinction. The contour levels are shown. The best fit equations are given (error in parentis). The distribution of Planck function along the extension (major diameter) (e) and compression (minor diameter) (f) of the cavity. The solid curves represent Gaussian (d), sine curve fitted (e, f) and linear fitted (b, h).

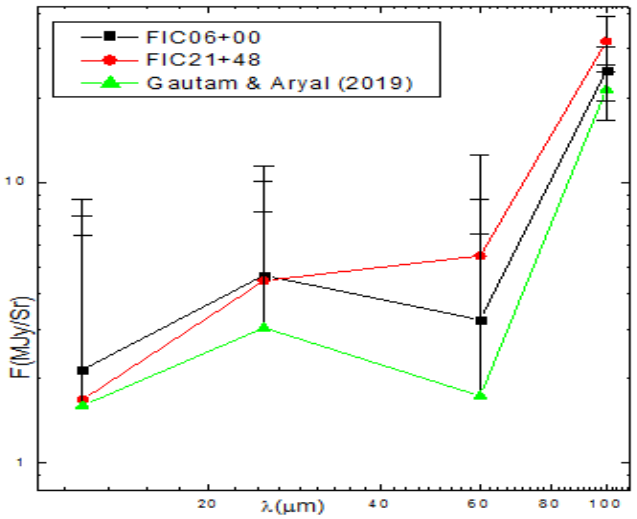


**Figure-3:** Spectral distributions of the two FIR cavities and a comparison with the far infrared cavity[17].

## Conclusion

Physical properties such as the dust color temperature, Planck function along the diameters, visual extinction and their distribution of two far infrared cavities located nearby AGB stars within $3.0^0$ radius at 60μm and 100μm IRAS maps were studied. Additionally, far infrared spectral distributions at 12 μm, 25μm, 60μm and 100μm were also analysed. Conclusions of this paper are summarised as follows:

The values of dust color temperature was found to lie in the range (20.5±1.2) K to (22.6±0.4) K. The contour map of dust color temperature and visual extinction showed that lower the temperature, higher the visual extinction and vice-versa. Both the cavities showed Gaussian like nature with positive skewness in the Gaussian fit of dust color temperature. A fluctuation in the distribution of Planck function along the major and minor diameters of the FIR cavities was noticed which suggests that the dusts might not be in the thermodynamic equilibrium locally. After sine curve fitting, dust particles were more or less oscillating sinusoidally. Product of visual extinction and dust color temperature was found to lie in the range $1.0\times10^{-4}$ to $1.2\times10^{-4}$ mag K. FIR spectral distribution showed a significant decrease in the flux density from 25μm to 60 μm in FIC06+00 cavity supported by KK-loops but continuous increase in flux density in case of the cavity FIC21+48.

## Acknowledgements

Authors are grateful to express their gratitude to the Department of Astro-Particle Physics, Innsbrck University, specially to Prof. R. Weinberger for invoking us to work on dusty environments around AGB stars. This research has made possible by the use of Sky View Virtual Observatory, Aladin v2.5 and NASA/IPAC extragalactic Database (NED). Authors would like to give special thanks to faculty member and staffs of Dept. of Physics Bhaktapur Multiple Campus, Tribhuvan University, Bhaktapurj, Nepal.

## References

**1.** Jones, T. W., Ney, E. P., & Stein, W. A. (1981). Pulsations Grain Condensation and Mass Loss in Long-Period Variable Stars. *The Astrophysical Journal*, 250, 324-326.

**2.** Bowen, G. H. (1988). The Mechanism of Mass Loss from Pulsating Cool Stars. *The Astrophysical Journal*, 329, 299 - 317.

**3.** Cassara, L. P., Piovan, L., Weiss, A., Salaris, M., & Chiosi, C. (2013). Detailed AGB evolutionary models and near-infrared colours of intermediate-age stellar populations: tests on star clusters. *Monthly Notices of the Royal Astronomical Society*, 436, 2824-2851.

**4.** Habing, H. J. (1996). Circumstellar envelopes and Asymptotic Giant Branch stars. *Astronomy and Astrophysics Reviews*, 7, 97-207.

**5.** Herwig, F. (2005). Evolution of Asymptotic Giant Branch Stars. *Annu. Rev. Astron. Astrophysics*, 43, 435-479.

**6.** Villaver, E., Segura, G. G. & Manchado, A. (2002). The Asymptotic Giant Branch. *The Astrophysical Journal*, 571, 880-900.

**7.** Suh, K.W & Kwon, Y.J. (2009). A Catalog of AGB Stars in IRAS PSC. *Journal of the Korean Astronomical Society*, 42, 81-91.

**8.** Aryal, B., Rajbahak, C., & Weinberger, R. (2010). A giant dusty bipolar structure around the planetary nebula ngc 1514. *Monthly Notices of the Royal Astronomical Society*, 402,1307-1312.

**9.** Aryal, B., Rajbahak, C., & Weinberger, R. (2009). Planetary nebulae NGC 6826 and NGC 2899: early aspherical mass loss? *Astrophysics and Space Science*, 323, 323-328.

**10.** Aryal, B., & Weinberger, R. (2006). A new large high latitude cone-like far-ir nebula. *Astronomy and Astrophysics*, 448, 213-219.

**11.** Jha, A. K., Aryal, B., & Weinberger, R. (2017). Study of dust color temperature and dust mass distributions of four far infrared loops. *Revista Mexicana de Astronomia y Astrofisica*, 53, 467-476.

**12.** Jha A. K. and Aryal B. (2018). Dust color temperature distribution of two far infrared cavities at iris and akari maps. *Journal of Astrophysics and Astronomy*, 39(2), 7-16.

**13.** Wood, D.O.S., Myers, P.C., & Daugherty, D.A. (1994). IRAS images of nearby dark clouds. *The Astrophysical Journal Supplement*, 95, 457-501.

**14.** Dupac, X., Bernard, J.P., Boudet, N., Giard, M., Lamarre, J.M., Meny, C., Pajot, F., Ristorcelli, I., Serra,G., Stepnik,

B. & Torre, J.P. (2003). Inverse Temperature Dependence of the Dust Submillimeter Spectral Index. *Astronomy & Astrophysics*, 404, L11-L15.

**15.** Schnee, S.L., Ridge, N.A., Goodman, A.A. & Jason, G.L. (2005). A Complete Look at the Use of IRAS Emission Maps to Estimate Extinction and Dust Temperature. *The Astrophysical Journal*, 634, 442-450.

**16.** Beichman, C.A., Wilson, R.W., Langer, W.D., & Goldsmith, P.F. (1988). Infrared limb brightening in the Barnard 5 cloud. *The Astrophysical Journal Letters*, 332, L81-L85.

**17.** Gautam, A. K., & Aryal, B. (2019). A study of low-latitude ($|l| < 10^0$) far infrared cavities. *Journal of Astrophysics and Astronomy*, 40, 16-26.

**18.** Weiland, J. L., Blitz, L., Dwek, E., Hauser, M. G., Magnani, L., & Rickard, L. J. (1986). Infrared cirrus and high-latitude molecular clouds. The Astrophysical Journal Letters, 306, L101-L104.